Published in final edited form as:
Photochem Photobiol. 2013 March ; 89(2): 326–331. doi:10.1111/php.12009.

Pyrazole-substituted Near-infrared Cyanine Dyes Exhibit pH-dependent Fluorescence Lifetime Properties

Hyeran Lee, **Mikhail Y. Berezin**, **Rui Tang**, **Natalia Zhegalova**, and **Samuel Achilefu***
Department of Radiology, Washington University, St. Louis, Missouri 63110, United States

Abstract

Near-infrared heptamethine cyanine dye is functionalized with pyrazole derivatives at the meso-position to induce pH-dependent photophysical properties. The presence of pyrazole unsubstituted at 1-position is essential to induce pH-dependent fluorescence intensity and lifetime changes of these dyes. Replacement of meso-chloro group of cyanine dye IR820 with ^{1}N-unsubstituted pyrazole resulted in the pH-dependent fluorescence lifetime changes from 0.93 ns in neutral media to 1.27 ns in acidic media in DMSO. Time resolved emission spectra (TRES) revealed that at lower pH, the pyrazole consists of fluorophores with two distinct lifetimes, which corresponds to pH sensitive and non-pH sensitive species. In contrast, ^{1}N-substituted pyrazoles do not exhibit pH response, suggesting excited state electron transfer as the mechanism of pH-dependent fluorescence lifetime sensitivity for this class of compounds.

INTRODUCTION

Fluorescent probes that can quantify small pH changes are useful for monitoring the pH of biological systems (1). Tissue pH imaging has been accomplished with diverse pH-sensitive fluorescent dyes and methods (2–5). These techniques mainly rely on the pH-dependent fluorescence intensity changes that are largely influenced by the pH probe concentration. On the contrary, the fluorescence lifetimes of fluorophores are intrinsic properties that are less sensitive to fluorophore concentration than fluorescence intensity measurements. Since the techniques used to determine fluorophore lifetimes inherently have fluorescence intensity information, lifetime measurements provide additional functional information that may not be readily accessible by conventional methods. For these reasons, lifetime-based techniques have been used to detect pH changes using different fluorescent indicators (6–15). A wide range of fluorescence lifetime sensors have been developed including visible fluorescein dyes (16), pH-sensitive organic dyes encapsulated in nanostructured matrix (17), or metal-ligand complexes (18).

Near-infrared (NIR) absorbing fluorescent probes with pH-dependent optical properties offer many advantages over visible dyes, such as low background signal from tissues or other biological samples. Due to their excellent photophysical properties and ease of synthetic modifications, NIR heptamethine cyanine dyes have been increasingly preferred over other fluorescent probes for pH sensing applications. Two major classes of these pH-sensitive dyes include norcyanine dyes with a pH responsive indolium nitrogen atom and ketocyanine dyes with keto-enol isomerization site at the meso-position of heptamethine dye (19–21). Recently, we reported barbituric acid-incorporated cyanine dyes to generate pH-dependent NIR dyes for biological applications (22). Although these dyes show good pH-dependent optical properties, their pKa values were too low for conventional biological applications (pKa~3.5).

*Correspondence to: Samuel Achilefu, PhD, Phone: 314 362 8599, Fax: 314 747 5191, achilefus@mir.wustl.edu.

We hypothesized that the introduction of the pH sensor at the meso position of the fluorophore will alter the fluorescence lifetime of the polymethine probe. This was based on our previous report that placement of an amine in close proximity to the fluorophore changes the fluorescence lifetime (23). Here, we report pH-dependent fluorescence lifetime properties of NIR pyrazole-substituted heptamethine cyanine dyes with pKa ~5 in the biologically relevant range.

MATERIALS AND METHODS

Materials

IR-820 and bovine serum albumin (>96%, lyophilized powder) were purchased from Sigma-Aldrich (St. Louis, MO). 1-Benzyl-1H-pyrazole-4-boronic acid, 3,5-dimethylpyrazole-4-boronic acid pinacol ester, and 1-isobutyl-1H-pyrazole-5-boronic acid pinacol ester were purchased from Boron Molecular (Research Triangle, NC). RP C18 Silica gel (17% carbon load) was purchased from Sorbent Technology (Sorbtech, Norcross, GA). C18 TLC plates Alugram RP-18W/UV_{254} were obtained from Macherey-Nagel (GmbH&Co., Germany).

Preparation of pH-sensitive probes

Pyrazole-substituted NIR dyes were prepared according to the modified published procedure (24). Briefly, the precursor chloro dye IR-820 (20 mg) was dissolved in oxygen-free water (5 mL; the reaction is summarized in Equation 1). An appropriate pyrazole derivative (2 eq.) such as pyrazole-substituted boronic acid (for dye **1**) or boronic esters (for dye **2** and **3**) in 1 mL of DMF was added along with $Pd(PPh_3)_4$ (3 mg). The reaction mixture was refluxed and the progress was monitored by TLC on RP C18 silica gel. The reaction was terminated when all IR820 dye was consumed (3 h for dye **2**, and 16 h for dyes **1** and **3**). The reaction mixture was then cooled to room temperature and filtered through Celite. Solvents were evaporated under vacuum and the residue was purified by column chromatography on RP C18 silica gel using water-methanol gradient elution. Fractions containing the desired product (determined by LCMS) were combined, the solvents were evaporated, and the residue was lyophilized. The resulting solid residue was re-dissolved in a small amount of methanol and triturated with diethyl ether. The precipitate was further washed with diethyl ether twice to afford pure dyes **1**-**3** as green powder.

Dye 1—Yield, 12%. ESI-MS (negative matrix), *m/z*: 949 (MH^+); ^{1}H NMR (400 MHz, $CDCl_3$) δ ppm: 7.97-7.92 (7H, m), 7.66-7.62 (6H, m), 7.57-7.53 (5H, m), 7.45-7.42 (3H, m), 6.35 (2H, d, *J*=14.4 Hz), 5.57 (2H, s), 4.19 (4H, m), 2.86 (4H, t, *J*=6.8 Hz), 2.71 (4H, m), 2.01-1.91 (10H, m), 1.47 (12H, s).) Abs/em (MeOH):λ_{max} = 800 nm, λ_{em} =821 nm.

Dye 2—Yield, 78%. ESI-MS (negative matrix), *m/z*: 914 (MH^+); ^{1}H NMR (400 MHz, $CDCl_3$) δ ppm: 8.04 (2H, d, *J*=8.8 Hz), 7.95-7.91 (4H, m), 7.74-7.66 (4H, m), 7.57-7.54 (4H, m), 7.41 (2H, t, *J*=7.4 Hz), 6.26 (2H, d, *J*=14 Hz), 4.21 (6H, m), 2.87 (4H, t, *J*=7 Hz), 2.72 (4H, m), 2.41 (1H, m, *J*=6.8Hz), 2.00-1.92 (10H, m), 1.67 (12H, s), 1.12 (6H, d, *J*=6.8 Hz); Abs/em (MeOH): λ_{max} =802 nm, λ_{em} =822 nm.

Dye 3—Yield, 97%. ESI-MS (negative matrix), *m/z*: 887 (MH^+); ^{1}H NMR (400 MHz, $CDCl_3$) δ ppm: 8.53 (2H, d, *J*=14 Hz), 8.24 (2H, d, *J*=8.4 Hz), 8.01-7.96 (4H, m), 7.66-7.60 (4H, m), 7.47 (2H, t, *J*=7.2 Hz), 6.35 (2H, d, *J*=14.4 Hz), 4.32 (4H, m), 2.89 (4H, t, *J*=6.8 Hz), 2.77 (4H, m), 2.17-1.92 (28H, m); Abs/em (MeOH):λ_{max} = 760 nm, λ_{em} = 770 nm, pH < 5; λ_{max} = 820 nm, λ_{em} = 824 nm, pH > 5.

Steady-state optical measurements

Absorption spectra were recorded on a DU 640 UV-visible spectrophotometer (Beckman Coulter, Brea, CA) and fluorescence spectra were recorded on a Fluorolog-3 spectrofluorometer (Horiba Jobin Yvon, Inc., Edison, NJ). All fluorescence measurements were conducted at room temperature and were recorded at excitation of 700 nm and emission scan from 715–950 nm.

For titrations, the compounds were pre-dissolved in MeOH maintaining the absorbance below 0.4 units at the maximum absorption. The methanolic solution was then either acidified with trifluoroacidic acid (TFA) or basified with triethylamine (TEA). The pH of the solution was measured after diluting with NaCl (0.1 M) solution (1:1 vol) to provide relatively constant ionic strength using Accumet pH meter AB15 (Fisher Sci. Pittsburgh, PA). At each pH point, absorption and fluorescence measurements were determined. The pKa value was calculated from the fluorescence intensity ratio between 770 nm and 820 nm emission peaks using sigmoidal dose-response curve fit implemented in Prism 5.0 software (GraphPad Software Inc., La Jolla, CA). The molar extinction coefficient was obtained using Beer's law at 0.1–0.6 μM concentration for each dye. The relative fluorescence quantum yields of the dye were determined at different pH using the equation:

$$\Phi_{F(x)} = (A_s/A_x)\,(F_x/F_s)\,(n_x/n_s)^2 \Phi_{F(s)}$$

where $\Phi_{F(X)}$ is the fluorescence quantum yield, A is the absorbance, F is the area under the emission curve, n is the refractive index of the solvents used in the measurement, and the subscripts s and x represent the reference and unknown parameters, respectively. Indocyanine green (ICG, Akorn, Inc. Decatur, IL) was used as a reference standard, which has a quantum yield of 0.09 in MeOH at 700 nm excitation (25).

Fluorescence lifetime measurements

Fluorescence lifetimes (FLT) were measured using time correlated single photon counting (TCSPC implemented in Fluorolog-3, Horiba Jobin Yvon) with a 700 nm excitation source NanoLed® (impulse repetition rate 1 MHz) at 90o to the PMT R928P detector (Hamamatsu Photonics, Japan). The dyes were dissolved in DMSO and the absorbance of the measured solutions was maintained below 0.15 at a 700 nm excitation wavelength. We chose DMSO as solvent for this study because it provides similar environment as the biological systems. The detector was set to 780 nm with a 26 nm bandpass and data were collected until the peak signal reached 10,000 counts. The details of the system have been published in a previous study (26). The instrument response function was obtained using a Rayleigh scatter of Ludox-40 (0.05% in MQ water; Sigma-Aldrich) in an acrylic transparent cuvette at 700 nm emission. Decay analysis software (DAS6 v6.1; Horiba) was used for lifetime calculations. The goodness of fit was judged by χ^2 values, Durbin–Watson parameters, as well as visual observations of fitted line, residuals, and autocorrelation functions. For titrations, the dyes were dissolved in DMSO and acidified with dilute trifluoroacetic acid (TFA) or basified with dilute triethylamine (TEA). The resulting DMSO solutions were diluted with 0.1 M NaCl aqueous solution (1:1 vol), the pH of the solution was measured (pH_m) and corrected for dilution using following formula (10):

$$\mathrm{pH} = -\log\left[10^{-\mathrm{pHm}}/2\right] \text{ (for acidic conditions)}$$
$$\mathrm{pH} = 14 - \log\left[10^{-(14-\mathrm{pHm})}/2\right] \text{ (for basic conditions)}$$

RESULTS AND DISCUSSION

Synthesis of pH-dependent fluorescence lifetime probes

Syntheses of pH-dependent pyrazole-substituted NIR cyanine dyes **1**-**3** are shown in Equation 1. Meso-pyrazole substituted dyes were obtained from commercially available chloro-substituted dye, IR-820, using modified published procedure (24). Under standard Suzuki-coupling conditions, the presence of common base required for these reactions promote decomposition of base-labile heptamethine cyanine dyes or the formation of by-products. These complications were circumvented by conducting the experiment in water/DMF mixture, which served as both a base and reaction solvent. The reaction mixture was purified by column chromatography on reversed phase (RP) silica gel and the precipitate formed after lyophilization of the combined fractions was recrystallized from MeOH/diethyl ether. The UV-Vis and LC-MS data are consistent with the expected features for dyes **1**-**3**.

Optical properties of pH-dependent lifetime probes

We determined the pH-dependent optical properties of the pyrazole-substituted cyanine dyes **1**-**3** by analyzing their absorption and fluorescence spectra in different pH mediums. Representative absorption and fluorescence spectra of pyrazole-substituted dye **1** are shown in Figure 1. The absorption spectra of this dye show a characteristic band broadening, which is typical of heptamethine cyanine dyes. A small hypsochromic shift (~5 nm) from the parent chloro dye, IR-820, was observed, indicating a direct C,C-coupling of the pyrazole moiety with cyanine framework according to the previous studies of our group (22, 24, 26). Similarly, the emission band is broad, with maximum emission peak at 817 nm. This small Stokes shift indicates that minimal amount of excitation energy is lost via excited state-reactions, solvent effect, complex formation, and/or energy transfer (27). The absorption and emission spectra of dye **1** suggests that dyes with benzyl group at the ^{1}N-position of pyrazole do not exhibit characteristic pH-dependent spectral properties within the range examined. A similar poor pH response was observed for dye **2**, which has ^{1}N-isobutyl substituent (not shown).

Interestingly, dye **3** exhibits pH-dependent optical properties, as shown in Figure 2. This dye shows a broad absorption band centered at 820 nm in neutral and basic media. At lower pH, a new band centered at 760 nm becomes evident in addition to the original band at 820 nm. The pH-dependent spectral properties of dye **3** are more evident in the emission spectra. Below pH 2.7, fluorescence intensity data exhibits a single emission peak at 770 nm. As pH increases, 770 nm peak becomes smaller with simultaneous increase of an additional emission peak at 824 nm. Above pH 5.7, emission peak at 770 nm disappears while emission peak at 824 nm becomes dominant. Fluorescence intensity at 770 nm in acidic media is 4 times greater than that at 824 nm with small Stokes shifts of 4–10 nm.

The pKa value of dye **3** was determined by fluorescence intensity ratio of 770 nm to 824 nm and was found to be 5.1 (Figure 3). Although it is evident that presence of free ^{1}N-H is essential to induce the pH-dependent spectral shift, it is also plausible that intense fluorescence band at 770 nm is caused by H-band fluorescence (see absorption spectra in Fig 3b, a small shoulder at 760 at low pH might indicate the presence of H-aggregation). Normally, H-aggregates do not fluoresce except that few merocyanines exhibit strong H-bands fluorescence (28). To further demonstrate that fluorescence shift is due to equilibrium between protonation-deprotonation of N-H substituents and not due to aggregation, the dye was allowed to bind albumin under neutral conditions. Albumin-bound dye is expected to be in a mono-form due to geometry constraints of the binding pocket. The aqueous albumin-dye complex was then treated with small amount of trifluoroacetic acid (TFA). As shown in Figure 3, it is evident that dye bound to albumin still exhibits hypsochromic shift in acidic

media from 820 nm, indicating the origin of highly fluorescent peak is due to protonation of the dye and not due to aggregation. However, the shift is relatively small in PBS from 820 nm to 790 nm compared to 820 nm to 770 nm in MeOH. This relatively small spectral shift is indicative that the dye was still bound to albumin.

Lifetime measurements and Time-resolved fluorescence

Fluorescence lifetime was measured in acidic, neutral and basic media in both methanol and DMSO solutions with excitation wavelength of 700 nm in all experiments. In acidic media, the lifetime was measured at 750 nm to measure the emission of the protonated species. In other cases the lifetime was measured at 820 nm which corresponds to neutral molecules. As can be seen in tables below, fluorescence lifetime exhibited pH-dependent properties at different solvents. In methanol solutions, fluorescence lifetime at pH 4 was determined to be 0.74 ns at 750 nm excitation wavelength while at higher pH fluorescence lifetime shifted to 0.50 ns at 820 nm excitation wavelength. As expected, fluorescence lifetime was longer in DMSO with values of 1.27 ns at pH 4.3 and 0.93 ns at pH 7.7. The fluorescence quantum yield of the dye **3** also changes at different pH consistent with the corresponding changes in the fluorescence lifetime.

Time resolved emission spectra (TRES)

From the steady-state fluorescence spectra of a pyrazole dye at low pH, it was not clear if the shoulder at 820-830 nm is part of the emission spectra or it belongs to a non-protonated species which predominate at higher pH values. From the steady-state fluorescence spectra of a pyrazole dye at low pH, it was not clear if the shoulder at 820-830 nm is part of the emission spectra or it belongs to a non-protonated species which predominate at higher pH. To answer this question and to resolve steady state fluorescence spectrum of **3** at low pH, we used TRES.

TRES is often used to identify individual components in a mixture of fluorophores with different fluorescent lifetimes. (27, 29) The method is analogous to time gated fluorescence recording, where the sample is excited with a pulse of light and emission spectrum is recorded after a certain time interval (time gate). Differences in the spectra of the sample after a short time gate and after a long-time gate indicate the presence of two or more components in the sample. The method allows identifying the individual components through their unique spectra as well as the number of components in the mixture. In TRES method, the full decays of the mixture are recorded at different wavelengths of emission. Instead of time gating, an orthogonal slice across a decay curve is made through a 3D dataset. Each slice provides a spectrum that corresponds to a specific time gate rendering TRES and Time gating fluorescence techniques equivalent

Briefly, the decay curve was measured at multiple emission wavelengths to construct a 3D data set of counts vs. time vs. wavelength. Then the 3D dataset was sliced orthogonally at three places to the time axis to produce three 2D spectra of counts vs. wavelength. The first slice was taken at the peak of the decay, another slice was taken at the tail, and the third one (a broad slice) was taken between the peak and the tail to average the signal. The slices were compared using a normalized scale. The slices clearly showed that at lower pH a pyrazole consists of two or more separate fluorophores, a pH sensitive and non-pH sensitive which might indicate that by the analogy with non-pH sensitive benzyl-pyrazole protonation at the ^{2}N-position leads to a non-pH sensitive compound, while protonation at the ^{1}N-position leads to a pH sensitive component (Figure 4).

Correlation of dye structures and spectral properties to determine site of pH sensor

There are two nitrogen centers on the pyrazole ring that can induce pH-sensitivity of the chromophore system. To determine the basis of pH sensitivity of dye **3**, we examined the correlation between the structures of pyrazole dyes **1-3** and their optical properties. Based on the spectral analysis, dyes with pyrazoles substituted in the 1-position with benzyl or isobutyl group does not exhibit noticeable spectral changes at different pH values. Although it is very plausible that equilibrium between protonation-deprotonation at ^{2}N-position still occur at lower pH, this does not produce apparent spectral changes. It is also clear that unsubstitution at ^{1}N-position is necessary to induce spectral changes at different pH values. From TRES analysis, two or more separate fluorophores coexist at pH 4, possibly $\mathbf{3H^+}$, **3**, and $\mathbf{3H^-}$ (Scheme 1). While equilibrium between $\mathbf{3H^+}$ and **3** (^{2}N-H dissociation) does not induce any spectral changes, equilibrium between **3** and $\mathbf{3H^-}$ produces pH-dependent spectral changes. Drastically low pKa of 5.1 for ^{1}N-H dissociation equilibrium of **3** compared to the typical pK_a of 14.21 for ^{1}N-H acidity of pyrazoles is due to the favorable delocalization of negative charge in the conjugate base across the cyanine molecular framework. Deprotonation of **3** results in the loss of net charge to give $\mathbf{3H_a^-}$ and its resonant forms $\mathbf{3H_b^-}$ and $\mathbf{3H_c^-}$.

CONCLUSION

Meso-pyrazole substituted NIR cyanine dyes have been prepared via modified Suzuki coupling method and their pH-dependent optical properties were investigated. Fluorescence intensity data indicated that dye unsubstituted at ^{1}N-position exhibited pH-sensitive spectral properties with an absorption maxima shift from 820 nm in neutral media to 760 nm in acidic media. pKa value obtained from ratiometric measurements of 760 nm/824 nm was found to be 5.1. Fluorescence lifetime data showed pH and solvent-dependent lifetime changes of dye **3** from 0.93 ns in neutral media to 1.27 ns in acidic media in DMSO. In methanol solution, fluorescence lifetime changed from 0.50 ns in neutral media to 0.74 ns in acidic media.

Acknowledgments

This study was supported in part by grants from the National Institutes of Health (NIBIB R01 EB007276 and EB008111).

References

1. Han J, Burgess K. Fluorescent indicators for intracellular pH. Chem Rev. 2010; 110:2709–2728. [PubMed: 19831417]
2. Mordon S, Devoisselle JM, Soulie S. Fluorescence spectroscopy of pH in vivo using a dual-emission fluorophore (C-SNAFL-1). J Photochem Photobiol B. 1995; 28:19–23. [PubMed: 7791002]
3. Sanders R, Draaijer A, Gerritsen HC, Houpt PM, Levine YK. Quantitative pH imaging in cells using confocal fluorescence lifetime imaging microscopy. Anal Biochem. 1995; 227:302–308. [PubMed: 7573951]
4. Whitaker JE, Haugland RP, Prendergast FG. Spectral and photophysical studies of benzo[c]xanthene dyes: dual emission pH sensors. Anal Biochem. 1991; 194:330–344. [PubMed: 1862936]
5. Hilderbrand SA, Kelly KA, Niedre M, Weissleder R. Near infrared fluorescence-based bacteriophage particles for ratiometric pH imaging. Bioconjug Chem. 2008; 19:1635–1639. [PubMed: 18666791]
6. Boens N, Qin W, Baruah M, De Borggraeve WM, Filarowski A, Smisdom N, Ameloot M, Crovetto L, Talavera EM, Alvarez-Pez JM. Rational design, synthesis, and spectroscopic and photophysical

properties of a visible-light-excitable, ratiometric, fluorescent near-neutral pH indicator based on BODIPY. Chemistry. 2011; 17:10924–10934. [PubMed: 21932233]

7. Kuwana E, Sevick-Muraca EM. Fluorescence lifetime spectroscopy for pH sensing in scattering media. Anal Chem. 2003; 75:4325–4329. [PubMed: 14632153]
8. Hassan M, Riley J, Chernomordik V, Smith P, Pursley R, Lee SB, Capala J, Gandjbakhche AH. Fluorescence lifetime imaging system for in vivo studies. Mol Imaging. 2007; 6:229–236. [PubMed: 17711778]
9. Hanson KM, Behne MJ, Barry NP, Mauro TM, Gratton E, Clegg RM. Two-photon fluorescence lifetime imaging of the skin stratum corneum pH gradient. Biophys J. 2002; 83:1682–1690. [PubMed: 12202391]
10. Berezin MY, Guo K, Akers W, Northdurft RE, Culver JP, Teng B, Vasalatiy O, Barbacow K, Gandjbakhche A, Griffiths GL, Achilefu S. Near-infrared fluorescence lifetime pH-sensitive probes. Biophys J. 2011; 100:2063–2072. [PubMed: 21504743]
11. Almutairi A, Guillaudeu SJ, Berezin MY, Achilefu S, Frechet JM. Biodegradable pH-sensing dendritic nanoprobes for near-infrared fluorescence lifetime and intensity imaging. J Am Chem Soc. 2008; 130:444–445. [PubMed: 18088125]
12. Baruah M, Qin W, Basaric N, De Borggraeve WM, Boens N. BODIPY-based hydroxyaryl derivatives as fluorescent pH probes. J Org Chem. 2005; 70:4152–4157. [PubMed: 15876108]
13. Baruah M, Qin W, Flors C, Hofkens J, Vallee RA, Beljonne D, Van der Auweraer M, De Borggraeve WM, Boens N. Solvent and pH dependent fluorescent properties of a dimethylaminostyryl borondipyrromethene dye in solution. J Phys Chem A. 2006; 110:5998–6009. [PubMed: 16671668]
14. Boens N, Qin W, Basaric N, Orte A, Talavera EM, Alvarez-Pez JM. Photophysics of the fluorescent pH indicator BCECF. J Phys Chem A. 2006; 110:9334–9343. [PubMed: 16869681]
15. Qin W, Baruah M, Van der Auweraer M, De Schryver FC, Boens N. Photophysical properties of borondipyrromethene analogues in solution. J Phys Chem A. 2005; 109:7371–7384. [PubMed: 16834104]
16. Szmacinski H, Lakowicz JR. Optical measurements of pH using fluorescence lifetimes and phase-modulation fluorometry. Anal Chem. 1993; 65:1668–1674. [PubMed: 8368522]
17. Amali AJ, Awwad NH, Rana RK, Patra D. Nanoparticle assembled microcapsules for application as pH and ammonia sensor. Anal Chim Acta. 2011; 708:75–83. [PubMed: 22093347]
18. Murtaza Z, Chang Q, Rao G, Lin H, Lakowicz JR. Long-lifetime metal-ligand pH probe. Anal Biochem. 1997; 247:216–222. [PubMed: 9177680]
19. Zhang Z, Achilefu S. Design, synthesis and evaluation of near-infrared fluorescent pH indicators in a physiologically relevant range. Chem Commun (Camb). 2005:5887–5889. [PubMed: 16317464]
20. Strekowski L, Mason JC, Lee H, Say M, Patonay G. Water-soluble pH-sensitive 2,6-bis(substituted ethylidene)-cyclohexanone/hydroxy cyanine dyes that absorb in the visible/near-infrared regions. J Heterocyclic Chem. 2004; 41:227–232.
21. Strekowski L, Mason JC, Say M, Lee H, Gupta R, Hojjat M. Novel synthetic route to pH-sensitive 2,6-bis(substituted ethylidene)cyclohexanone/hydroxycyanine dyes that absorb in the visible/near-infrared regions. Heterocycl Commun. 2005; 11:129–134.
22. Lee H, Berezin MY, Guo K, Kao J, Achilefu S. Near-infrared fluorescent pH-sensitive probes via unexpected barbituric acid mediated synthesis. Org Lett. 2009; 11:29–32. [PubMed: 19061361]
23. Berezin MY, Kao J, Achilefu S. pH-dependent optical properties of synthetic fluorescent imidazoles. Chemistry. 2009; 15:3560–3566. [PubMed: 19212987]
24. Lee H, Mason JC, Achilefu S. Heptamethine cyanine dyes with a robust C-C bond at the central position of the chromophore. J Org Chem. 2006; 71:7862–7865. [PubMed: 16995699]
25. Benson RC, Kues HA. Fluorescence properties of indocyanine green as related to angiography. Phys Med Biol. 1978; 23:159–163. [PubMed: 635011]
26. Lee H, Berezin MY, Henary M, Strekowski L, Achilefu S. Fluorescence lifetime properties of near-infrared cyanine dyes in relation to their structures. J Photochem Photobiol A Chem. 2008; 200:438–444. [PubMed: 20016664]
27. Lakowicz, JR. Principles of Fluorescence Spectroscopy. Springer Science; New York: 2006.

28. Rosch U, Yao S, Wortmann R, Wurthner F. Fluoresceut H-aggregates of merocyanine dyes. Angew Chem Int Edit. 2006; 45:7026–7030.

29. Zhang Z, Berezin MY, Kao JL, d'Avignon A, Bai M, Achilefu S. Near-infrared dichromic fluorescent carbocyanine molecules. Angew Chem Int Ed Engl. 2008; 47:3584–3587. [PubMed: 18386274]

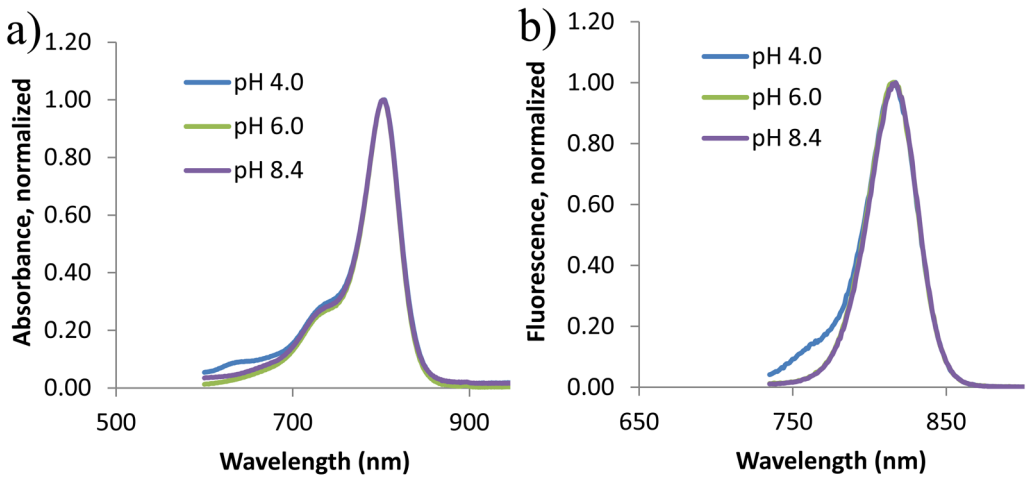

Figure 1.

Normalized absorption (a) and fluorescence spectra (b) of compound **1** in acidic, neutral and basic media of methanol solution. The emission spectra of the sample were taken with 720 nm excitation wavelength and collected from 735 nm to 900 nm.

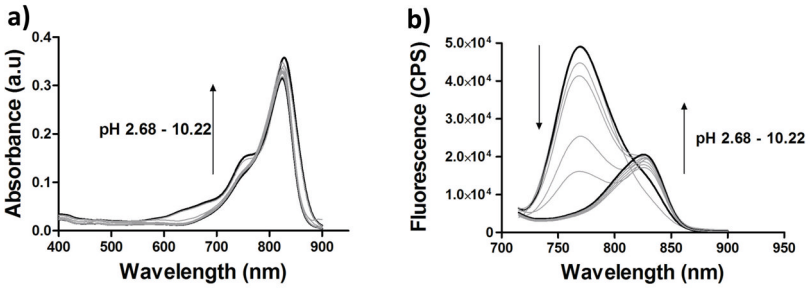

Figure 2.

Absorption (a) and fluorescence spectra (b) of compound **3** at different pH values. The emission spectra were collected from 715 nm to 900 nm with a 700 nm excitation wavelength.

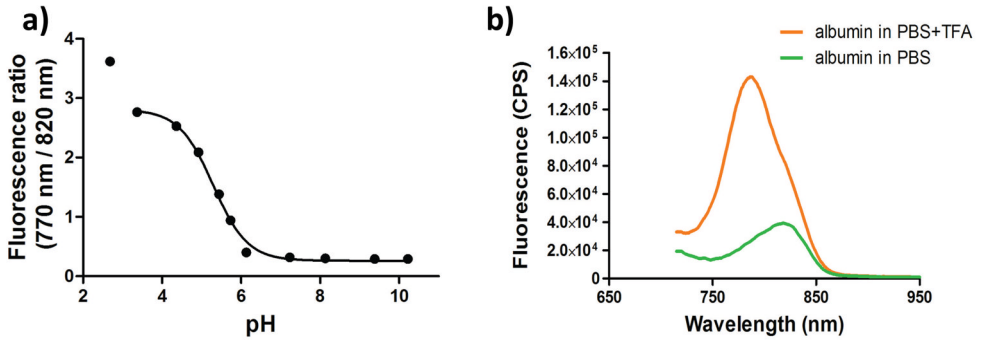

Figure 3.

(a) pKa titration curve expressed as a fluorescence intensity ratio of 770 nm to 820 nm at different pH values. Calculated pKa = 5.1 ± 1.3. (b) Fluorescence spectra of dye **3** bound to albumin in acidic and neutral media. Fluorescence intensity show sharp increase at 790 nm in acidic media.

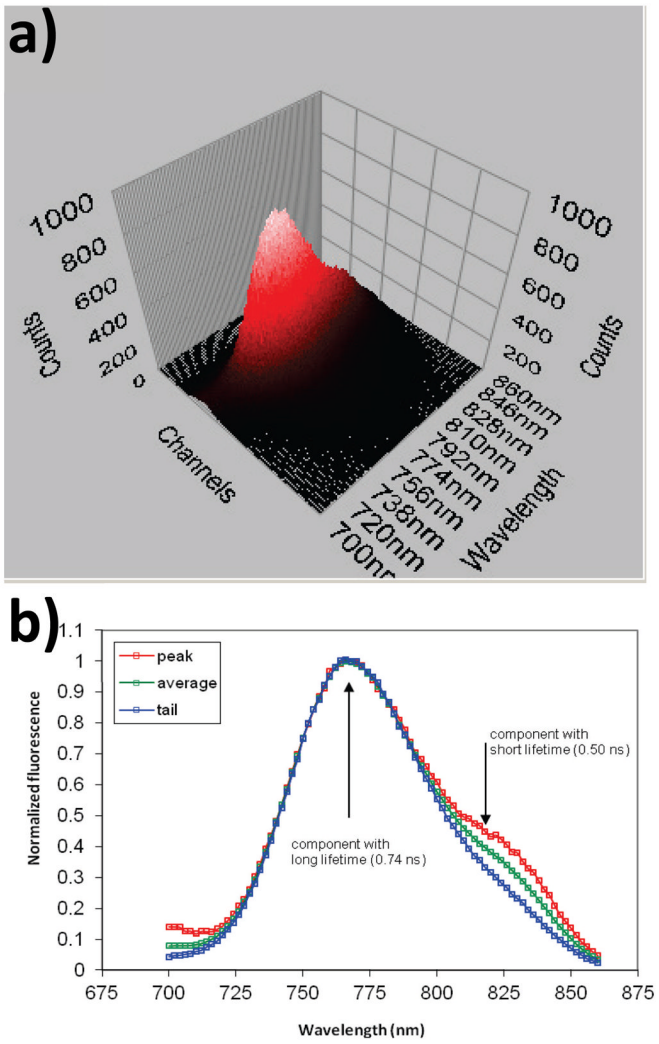

Figure 4.

(a) 3D TRES spectrum of dye **3** in methanol solution at pH=4.0, the arrows show the directions of slices. Red arrow – at the peak of the decay (short lived component), blue – at the tail of the decay (long lived component). (b) The 2D slices obtained are normalized and show that the long lifetime component does not have a shoulder, indicating that it belongs to two distinct fluorophores in solution, excitation 700 nm.

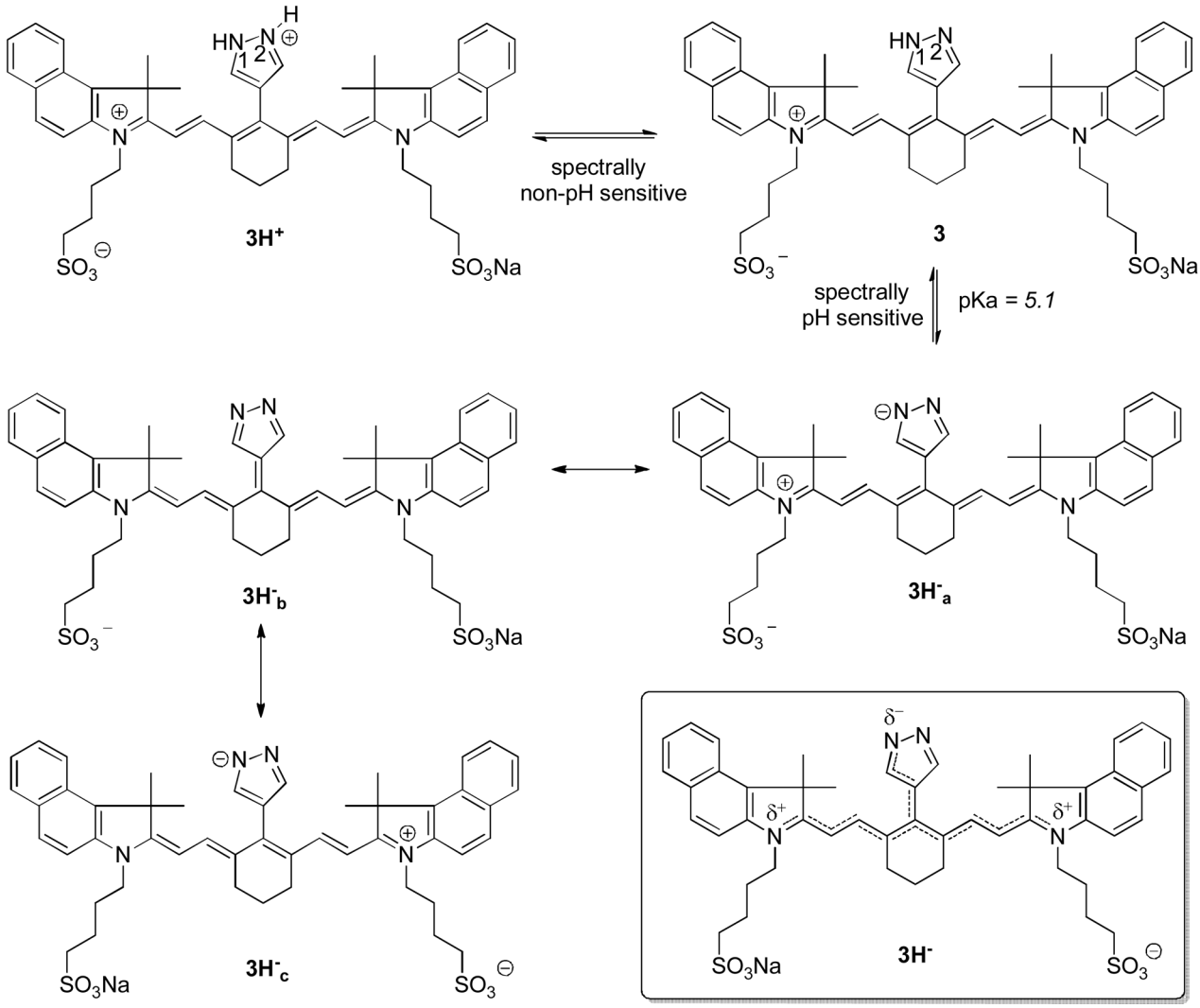

Scheme 1.
Proposed dissociation equilibrium of **3** in acidic, neutral and basic media

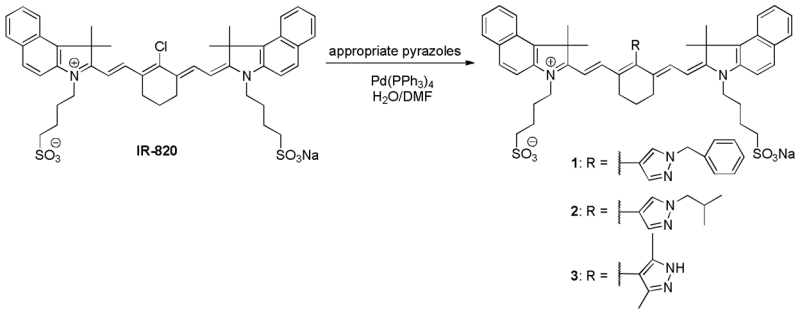

Equation 1.
Synthesis of Pyrazole-substituted Cyanine Dyes **1**-**3**

Table 1

Fluorescence lifetime properties of dye **3** in MeOH and DMSO.

In methanol:					
pH	**Monitoring wavelength**	**Lifetime, ns**	**Fractional contribution, %**	χ^2	**Quantum yield**
4.0	750	0.74	97	1.13	0.028
6.0	820	0.49	88	1.10	0.009
8.4	820	0.50	90	1.07	0.008

In DMSO:				
pH	**Monitoring wavelength**	**Lifetime, ns**	**Fractional contribution, %**	χ^2
4.3	750	1.27	103	1.05
5.7	820	1.04	90	1.10
7.7	820	0.93	88	1.07